From image analysis to damage constitutive law identification

S. Roux[a] and F. Hild[b]

Based on digital images of a tested sample, taken at different stages of loading, displacement fields are measured by using digital image correlation. The technique used here directly provides continuous displacement fields decomposed onto finite elements. From the latter, the equilibrium gap method allows one to estimate a scalar damage field over the same region of interest. Last, under the assumption of a unique constitutive law, the damage growth law is directly estimated from a series of displacement data. This procedure is illustrated on an experimental test case, namely a composite plate whose polymer matrix is reinforced with glass fibres, under equibiaxial tension loading.

Keywords: Digital Image Correlation, Damage, Identification

1. Introduction

The accurate description of the mechanical behaviour of composite materials, whose importance is not to be advocated for, usually requires a lengthy procedure, from the preparation of a series of experiments under different loading conditions, the accurate measurements of displacements and forces, the numerical modelling of the mechanical behaviour for different sets of constitutive parameters, the definition and extraction of observables to be compared with experimental ones, and iterations of the numerical modelling in order to reach a good agreement. Two major steps are limiting factors. The first one is the definition of observables, which should be robust enough to be accessible experimentally in a reliable way, and yet sensitive enough to discriminate different constitutive parameters. At this stage, only few pieces of information are typically used, and hence the identification procedure may not be as accurate as the quality of experiments would allow. Second, the iteration over different constitutive parameters requires several computations of a full non-linear problem, which may be long and costly.

Through the combination of recent advances in two techniques, a novel procedure is presented, which allows for the direct evaluation of constitutive parameters of a damage law from digital images taken at different stages of loading, without any additional data other than the Poisson's ratio of the undamaged material. These recent developments concern:

- First the measurement of full displacement fields from digital image correlation, which is formulated in such a way that it gives access to the displacement field decomposed over a basis of continuous functions. Many choices are possible, including for instance finite element kinematics. The latter choice (specifically Q4P1 elements, i.e., bi-linear functions of the coordinates over a square domain) is suited to the subsequent analysis.
- Second, the evaluation of a (potentially heterogeneous) field of elastic moduli, which accounts for the observed displacement field. The approach used herein is the "equilibrium gap" method (EGM). Its precise implementation differs slightly from the original presentation of Claire et al.,[1] which exploited a specific form based on Q8 elements for displacements. In the present version, the damage field is decomposed over an independent grid, which is typically coarser than that of the measured displacement field, in order to provide for a regularization called for by measurement uncertainties. This regularization implies a smooth spatial variation of damage, which

[a] Surface du Verre et Interfaces, UMR CNRS/Saint-Gobain, 39 quai Lucien Lefranc, F-93303 Aubervilliers cedex, France. (stephane.roux@saint-gobain.com)
[b] LMT-Cachan, 61 avenue du Président Wilson, F-94235 Cachan Cedex, France. (francois.hild@lmt.ens-cachan.fr)

may constitute a limitation for advanced damage where localization or macro-crack may occur.

Based on these two developments, the route is open for the identification of a damage law, which can be seen as a different kind of regularization. The assumption proposed here is that damage is only determined by an equivalent scalar strain, ε_{eq}. The latter growth is written under the form of a smooth law that does not prevent the occurrence of localized modes with sharp gradients. In that case, the damage variation is performed at the scale of the elements used for the displacement measurement. The quality of this determination is evaluated by re-computing the displacement field within the domain based on the damage parameters, and by comparing it to the measured field. As compared to the previously mentioned limitations, let us emphasize that:

- The entire kinematics is taken into account, so that no information is lost.
- Constitutive parameters (in the damage growth law) are obtained directly in one step without having to resort to heavy computations.
- An entire series of images can be considered simultaneously since the growth law should be the same at any stage of loading.

2. Experimental case study

The considered material is a vinylester based matrix that is reinforced by an isotropic distribution of short E-glass fibres. A thin plate made out of this material is prepared as a cross with wide arms, and subjected to biaxial tension. The white surface of the test piece is sprayed with black paint so as to produce a fine random texture, which is needed for the displacement field analysis.

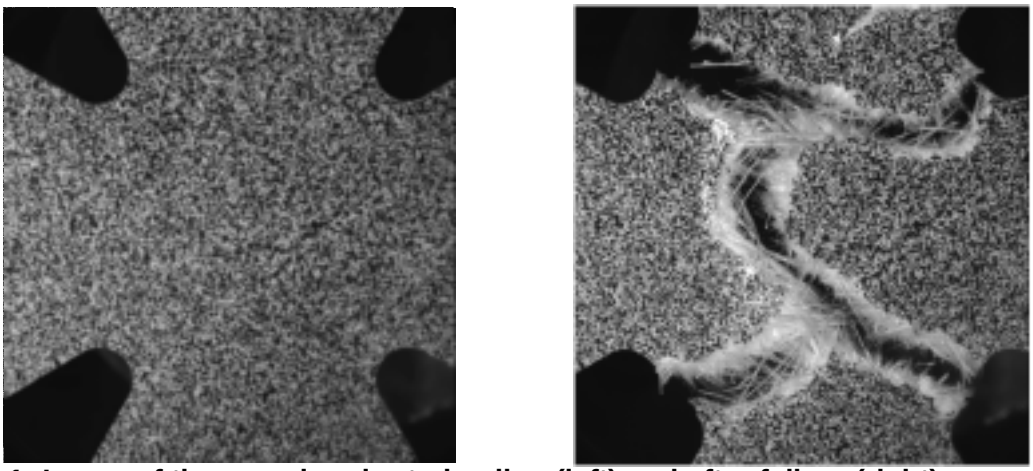

Figure 1: Image of the sample prior to loading (left) and after failure (right)

Digital images of the surface (1016 $\times$ 1008 pixels), using 256 grey levels (8-bit depth) are taken for every 1 kN load increment up to complete failure, which occurred for 11.1 kN. Thus 11 images are available for the analysis. The physical size of one pixel is 67 μm. Full details concerning this experiment can be found in Hild et al.[2] In the sequel, this experiment is used to illustrate the results that are achieved.

3. Image correlation technique

3.1 Principle

Digital image correlation is already a mature field in solid mechanics[3]. We only discuss here some recent advances. Let us introduce $f(\mathbf{x})$ and $g(\mathbf{x})$ the grey level images of respectively a reference and a deformed state. The image f should show a rather fine texture, which is the raw surface of the material if it is heterogeneous enough, or if the surface has significant patterns (e.g. roughness of the surface). Otherwise, an artificial texture is obtained by paint

spraying in order to achieve a small correlation length and a good contrast such as the one presented in Fig. 1.
The surface features are assumed to follow passively the displacement field of the test sample itself. Moreover, the thin plate geometry is chosen so that plane stress conditions are fulfilled. The mathematical formulation of this hypothesis (called "optical flow conservation") is

$$g(\mathbf{x}) = f(\mathbf{x}+\mathbf{U}(\mathbf{x})) \quad (1)$$

where $\mathbf{U}(\mathbf{x})$ is the sought displacement field. The issue is to estimate the latter from known f and g. For an arbitrary displacement, this problem is ill-posed. Regularization is introduced by searching $\mathbf{U}(\mathbf{x})$ in a subspace of functions

$$\mathbf{U}(\mathbf{x}) = \sum_n a_n \mathbf{\Phi}_n(\mathbf{x}) \quad (2)$$

Many choices are possible for $\mathbf{\Phi}$, and have been used successfully in the past (finite elements[4], Fourier functions, cubic splines, solution of an elastic problem[5], including cracks[6]). In the following example, finite element Q4P1 will be used (the elementary shape functions are $(1\pm x)(1\pm y)$ over the $[-1;1]^2$ square).
The unknown coefficients $\{a_n\}$ are searched for through the minimization of the quadratic difference

$$\mathrm{T}(a_n) = \iint \left[g(\mathbf{x}) - f\left(\mathbf{x} + \Sigma_n a_n \mathbf{\Phi}_n\right) \right]^2 d\mathbf{x} \quad (3)$$

Moreover, it is assumed that the displacement magnitude is small compared with the correlation length of the texture so that a first order Taylor expansion is legitimate. This turns the T functional into a simple quadratic form

$$\mathrm{T}_{lin}(a_n) = \iint \left[g(\mathbf{x}) - f(\mathbf{x}) - \Sigma_n a_n \mathbf{\Phi}_n \nabla f \right]^2 d\mathbf{x} \quad (4)$$

The latter assumption is very limiting, since one does not know a priori if it is fulfilled. However, both images are easily coarsened so that the correlation length is artificially extended while the displacement remains unchanged. There exist many ways of performing this coarsening, the simplest consists in averaging four pixels into one, and repeating this operation as many times as needed and works nicely.[7] This procedure is called multiscale. Once the displacements are determined at the coarser level, the deformed image is corrected and the same procedure is repeated with a finer image down to the original one.
The minimization of the quadratic form T_{lin} leads to a linear system in a_n, which is solved using standard procedures.[3]

3.2 Application

For the tested composite sample, at each stage the displacement field is determined from the comparison of the reference image (unloaded sample) and the current image. We only show in Fig. 2 the displacement field for the last image (11), for which crack initiation is guessed in the left hand top corner, because of the steep gradient in displacements.

A series of 11 such fields is obtained and will be used in the sequel. The typical uncertainty of the displacement measurement is of order 0.01 pixel, or in physical units less than 0.7 μm. As a result, the displacement is defined at the nodes of a regular grid of size 67×66. Note that in the four corners of the image, where the sample has been cut out, the displacement nodes are masked (see Fig. 2).

4. Identification

4.1 Principle

The following step consists in determining a field of elastic properties that accounts for the displacement field at each stage of loading. Let us first propose a simple modelling of damage as a scalar parameter, $D(\mathbf{x})$, such that the Young's modulus is reduced to $(1\text{-}D)E_0$, from its initial value E_0 while the Poisson's ratio, ν, remains unaltered.

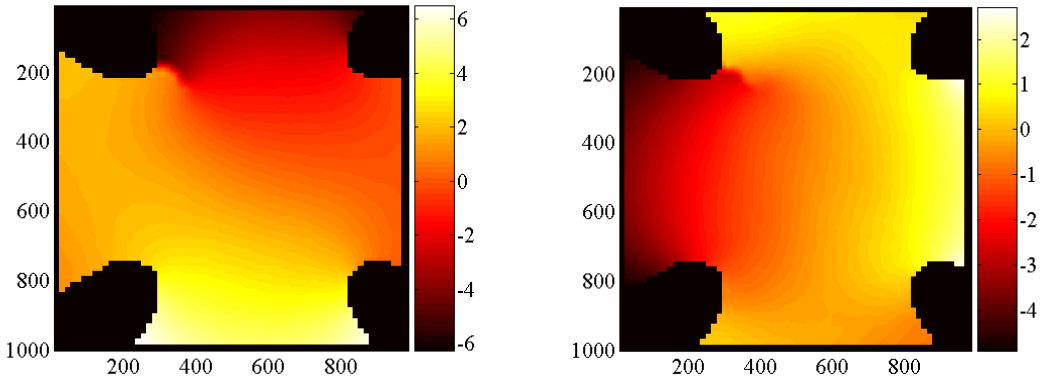

Figure 2: Vertical (left) and horizontal (right) component of the displacement field obtained from a Q4P1 decomposition with an element size equal to 16 pixels. The physical size of one pixel is 67 µm.

The spirit of the equilibrium gap method[1] is to exploit the equilibrium equation

$$\mathrm{div}\left[(1-D(\mathbf{x}))\mathbf{C}_0\varepsilon(\mathbf{U})\right]=0 \qquad (5)$$

written here in the absence of body forces. The strain ε is computed here from the known displacement field, and $\mathbf{C}_0$ is the Hooke's tensor of the virgin material. The damage, $D(\mathbf{x})$, is to be determined.
Since the displacement field is naturally decomposed over a finite element basis, we resort to the corresponding discretization of the "equilibrium gap", namely

$$(1-D)_m K_{ijm} U_j = 0 \qquad (6)$$

where K_{ijm} is the elementary rigidity matrix of the undamaged element m relating displacement component U_j to the nodal force F_i (whose sum over all element is equal to 0 for inner nodes). The rigidity matrix is linearly dependent upon the stiffness reduction $(1\text{-}D)$. Let us note that for more complex (e.g. anisotropic) damage models, this property may be violated, however still the same concept may be applied at the expense of a suited treatment of this non-linearity.
As can be seen from Eq. (6), since no static information is used (the second member is vanishing at all inner nodes), the $(1\text{-}D)$ field is determined up to an arbitrary scale factor. This is the price to pay for limiting the analysis to the knowledge of kinematic data only. The formulation is complemented by imposing arbitrarily that the average $(1\text{-}D)$ is equal to a constant. This is achieved by using a Lagrange multiplier or by eliminating one damage value.

Here again, for arbitrary damage fields, the problem is ill-posed and some regularization is called for. The most straightforward approach is to search for the "best" solution for the D-field in a subspace of smoothly varying fields in space. Finite elements Q4P1 are used in the

following, with however a grid that is independent of (and coarser from) the measurement mesh. Hence, we introduce shape functions N_{im} that provide the weight of the centre of an element m for the ith basis function, so that

$$(1-D)_m = N_{mi} b_i \tag{7}$$

This regularization limits the number of degrees of freedom and hence the damage field is obtained through the minimization of the functional

$$W(b) = \sum_j \left(\sum_{mi} L_{jm} N_{mi} b_i \right)^2 - \lambda \sum_{mi} N_{mi} b_i \tag{8}$$

where $L_{jm}=K_{ijm}U_i$, and λ is the Lagrange multiplier of the average damage constraint. The minimization of the functional W results in a linear problem that provides the b amplitudes, and thus from Eq. (7), the damage value in each element.
Let us note that in contrast with the original presentation of this method in Claire et al.,[1] the (1-D) variable and not its logarithm is used. Although the latter choice is more satisfactory in some respects (e.g., positivity of (1-D) is guaranteed), a linear formulation is generically obtained in discretized models only for nodes that are shared by two elements. This was possible using Q8 elements but only half of the nodes were considered. The logarithmic form may still be used but then the system is non-linear. The simplicity of the linearity has a drawback, namely the minimization of W may provide damage values greater than 1, and hence negative stiffnesses. Let us also underline that the present formulation allows one to disconnect the discretization of the damage field from that of the displacement field.

4.2 Application

Let us consider the final stage of damage as obtained with a coarse mesh (10 x 10 elements) and a finer one (20 x 20 elements) for the damage field.

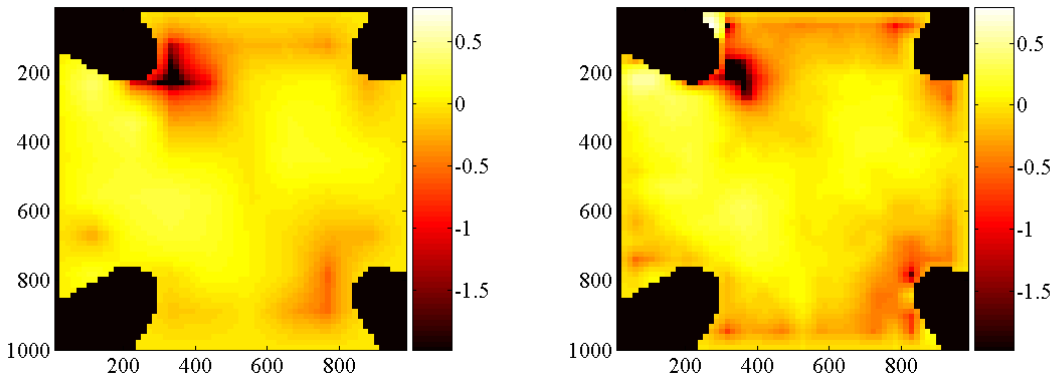

Figure 3: Map of $\log_{10}(1-D)$ obtained for a coarse (10 x 10) and fine (20 x 20) mesh.

Let us mention that in both cases, the stiffness reached a negative value at the top left corner (–0.02 and –0.3 respectively for the coarse and fine mesh). This value has been artificially reset to 0.01. We note a satisfactory agreement between both determinations, with a clear detection of crack initiation.

In order to evaluate the quality of the obtained damage map, it is possible to resort to a standard elastic computation based on the determined stiffness and using Dirichlet boundary conditions, i.e. imposing the displacement field on the boundary of the considered domain.

The computed displacement field is then to be compared with the measured one as shown in Fig. 4. A good agreement between both fields is observed from this figure. In order to quantify the agreement, the following dimensionless "residual" is defined: it is the standard deviation of the difference between identified and measured displacement field, normalized by the standard deviation of the measured displacement field. In the present case, for a fine grid (20x20), this residual amounts to 14%.

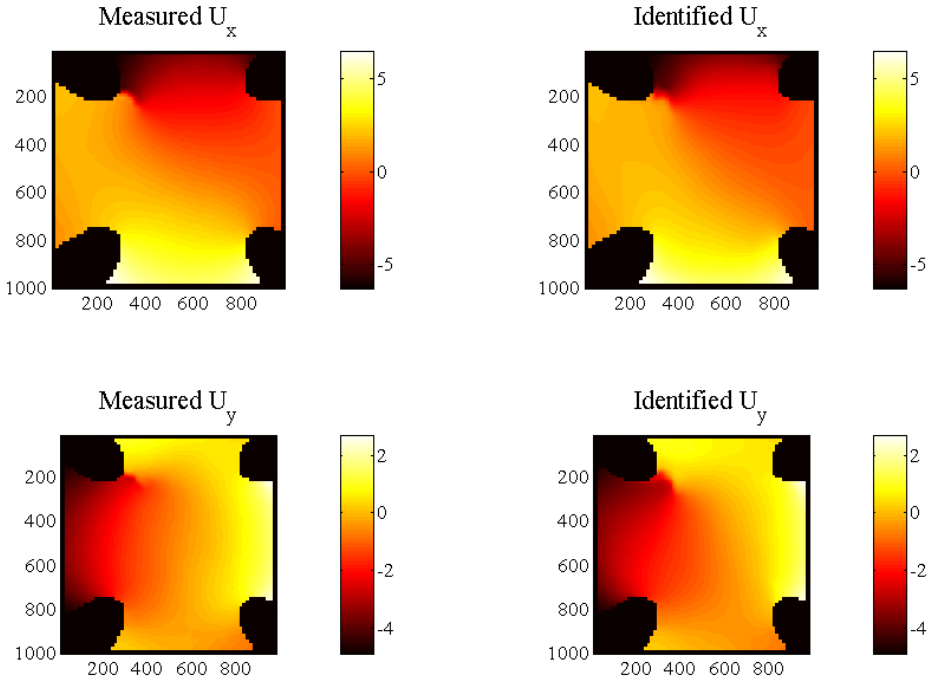

Figure 4: Comparison between measured (left) and recomputed (right) displacements from the identified damage field (fine grid 20 x 20).

5. Identification of a damage law

Identification has been thoroughly studied using various strategies. An important and successful one made use of the constitutive equation error[8910], including application to the estimate of damage field.[11] Virtual fields[1213] is an alternative method, which may be extended to heterogeneous damage fields. The reciprocity gap is yet another approach design to address damage or cracks inside an elastic medium[14]. We follow here a route closely related to the approach presented in Ref.[15], based on the equilibrium gap method.

5.1 Principle

Based on the previous results of the equilibrium gap method, it is tempting to go one step further, and identify a complete damage law. This can be seen as a different kind of regularization, where the local strain determines the damage level rather than its location in space. The scalar damage, which has been introduced above, is derived from a free energy density, ψ, expression

$$\psi = \frac{1}{2}(1-D)\varepsilon : \mathbf{C}_0 : \varepsilon \qquad (9)$$

where the damage variable is a function of its conjugate "force", the damage energy release rate density $Y = -\partial\psi / \partial D$. The latter is expressed by using an equivalent strain

$\varepsilon_{eq}^2 = 2Y / E_0$. The new regularization consists in expressing the dependence of D with respect to $2Y / E_0$ as a combination of different functions

$$D_m = \sum_n c_n f_n(2Y_m / E_0) \tag{10}$$

Moreover, if the additional constraint is considered, namely $f_n(2Y_m / E_0)$ = 0, the free stress scale degeneracy mentioned earlier vanishes, and thus the extra rule of imposing an average value for the stiffness is no longer needed. Let us introduce the matrix P_{mn} = $f_n(2Y_m / E_0)$ from which the quadratic equilibrium gap is minimized. The new functional reads

$$Z(c) = \sum_j \left(\sum_{mn} L_{jm} P_{mn} c_n - \sum_i L_{ji} \right)^2 \tag{11}$$

thus with a similar structure as W. Minimization leads again to a linear system, which provides directly the damage growth law thanks to Eq. (10).
Let us underline a novel feature of this formulation. Since the damage law should rule all states of damage, the same law should be determined at any stage of loading. Therefore, all Z functionals computed for different images are summed before proceeding to the minimization it self.

5.2 Application

The same experiments are used again. For the damage law, the following test functions are selected

$$f_n(x) = 1 - \exp(-x / x_n) \tag{12}$$

with a very small number of test functions, n = 2, and x_1 = 0.001 and x_2 = 0.005.

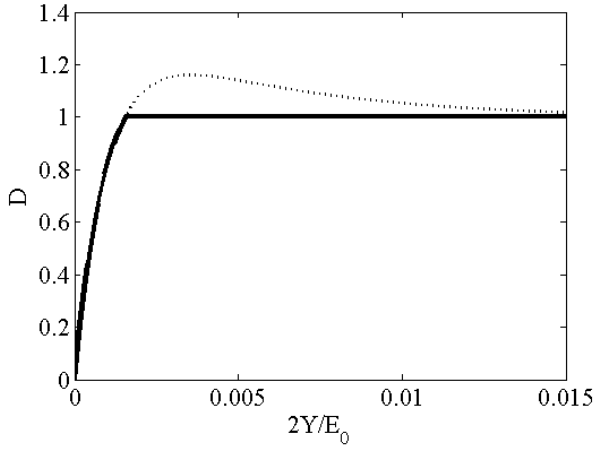

Figure 5: Identified damage law (dotted curve), which is truncated at D = 1 (bold curve).

As mentioned earlier, nothing prevents the damage parameter to exceed 1 as the problem is formulated. This is observed in Fig. 5 where the limit is violated, albeit by a small amount. Therefore the resulting damage law is truncated.
The distribution of the damage field based on this law is shown in Fig. 6 at the final stage. To reveal the small damage levels that occur away from the crack initiation zone, the map of $\log_{10}(D)$ is shown. This differs from Fig. 3 in which $\log_{10}(1\text{-}D)$ is shown.

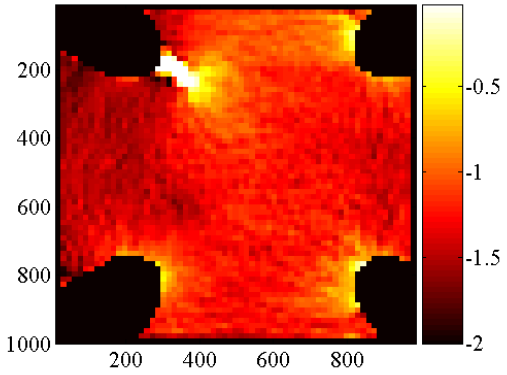

Figure 6: Map of $\log_{10}(D)$ at the final stage of loading.

The validity of the result is evaluated, as in the last section, by performing an elastic computation of the displacement field with Dirichlet boundary conditions. The comparison with measured displacements is now excellent. The dimensionless residual normalized standard deviation of the displacement difference between measured and identified fields) is now reduced to 5%.

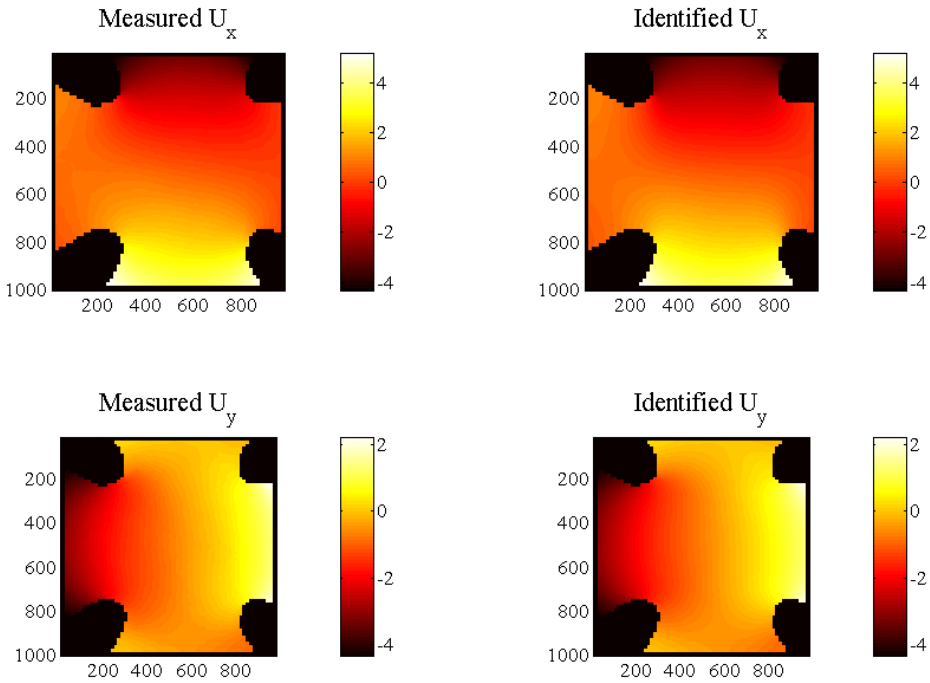

Figure 7: Comparison between measured (left) and recomputed (right) displacement field based on the identified damage law.

6. Conclusions

We have shown developments of digital image correlation techniques that allow one to bridge the gap between experiments and numerical modelling with the full benefit of full field measurements. Let us stress that the final damage law is obtained by using only a few images taken from a single test. Moreover, this determination is strongly influenced by the most severe damage states (last image) that emphasize the fact that heterogeneous tests are much more informative than homogeneous ones.
The simplicity and performance of this approach is, from our point of view, only a limited illustration of a technique that has a considerable potential, far beyond the present case study.

References

[1] D. Claire, F. Hild and S. Roux (2004) A finite element formulation to identify damage fields: The equilibrium gap method. Int. J. Num. Meth. Engng. **61** [2], 189-208.

[2] F. Hild, J.-N. Périé and M. Coret (1999) Mesure de champs de déplacements 2D par intercorrélation d'images : CORRELI^{2D}. Internal report **230**, LMT-Cachan.

[3] P. K. Rastogi (2000), edt., Photomechanics, (Springer, Berlin (Germany))

[4] G. Besnard, F. Hild and S. Roux (2006) "Finite-element" displacement fields analysis from digital images: Application to Portevin-Le Châtelier bands. Exp. Mech. [in press].

[5] F. Hild and S. Roux (2006) Digital image correlation: from measurement to identification of elastic properties - A review. Strain **42**, 69-80.

[6] S. Roux and F. Hild (2006) Stress intensity factor measurements from digital image correlation: post-processing and integrated approaches. Int. J. Fract. [in press].

[7] F. Hild, B. Raka, M. Baudequin, S. Roux and F. Cantelaube (2002) Multi-Scale Displacement Field Measurements of Compressed Mineral Wool Samples by Digital Image Correlation. Appl. Optics **IP 41** [32], 6815-6828.

[8] P. Ladevèze (1975) Comparaison de modèles de milieux continus, (thèse d'Etat, Université Paris 6). See also P. Ladevèze (1983) Updating of Complex Structure Models, (Aérospatiale, les Mureaux (France), technical report 33.11.01.4).

[9] R. V. Kohn and B. D. Lowe, (1988) A Variational Method for Parameter Identification, Math. Mod. Num. Ana. **22**, 119-158.

[10] H. D. Bui and A. Constantinescu (2000) Spatial localization of the error of constitutive law for the identification of defects in elastic solids, Arch. Mech.\/ **52**, 511-522.

[11] G. Geymonat, F. Hild and S. Pagano, (2002) Identification of elastic parameters by displacement field measurement, C. R. Mecanique **330**, 403-408.

[12] M. Grédiac (1989) Principe des travaux virtuels et identification, C. R. Acad Sci. Paris **309** [Série II] 1-5.

[13] M. Grédiac (2004) The use of full-field measurement methods in composite material characterization: interest and limitations, Composites: Part A **35**, 751-761.

[14] S. Andrieux, A. B. Abda and H. D. Bui, (1997) Sur l'identification de fissures planes via le concept d'écart à la réciprocité, C. R. Acad. Sci. Paris Série I, **324**,1431-1438.

[15] D. Claire, F. Hild and S. Roux (2006) Identification of a Damage Law Using Full-Field Displacement Measurements, Int. J. Dam. Mech. [in press]